

# Microstructure, Defects, and Reliability of Mixed Pb-Free/Sn-Pb Assemblies

POLINA SNUGOVSKY,<sup>1,2</sup> HEATHER McCORMICK,<sup>1</sup> SIMIN BAGHERI,<sup>1</sup>  
ZOHREH BAGHERI,<sup>1</sup> CRAIG HAMILTON,<sup>1</sup> and MARIANNE ROMANSKY<sup>1</sup>

1.—Celestica, 844 Don Mills Road, Toronto, ON, M3C 1V7, Canada. 2.—e-mail: polina@celestica.com

The results of an intensive reliability study on Pb-free ball grid array (BGA)/Sn-Pb solder assemblies as well as some lessons learnt dealing with mixed assembly production at Celestica are described in this paper. In the reliability study, four types of Pb-free ball grid array components were assembled on test vehicles using the Sn-Pb eutectic solder and typical Sn-Pb reflow profiles with 205°C to 220°C peak temperatures. Accelerated thermal cycling (ATC) was conducted at 0°C to 100°C. The influence of the microstructure on Weibull plot parameters and the failure mode will be shown. Interconnect defects such as nonuniform phase distribution, low-melting structure accumulation, and void formation are discussed. Recommendations on mixed assembly and rework parameters are given.

**Key words:** Pb-free components/Sn-Pb solder mixed assembly, microstructure, reliability, backward compatibility

## INTRODUCTION

The global transition to Pb-free solder impacts even industries and companies that are exempted or excluded from the Restriction of Hazardous Substances (RoHS) legislation. Component manufacturers have already switched to and are currently delivering components with Pb-free finishes. High-performance and high-reliability products with long lifetime and field rework or repair requirements need to accommodate this transition to lead-free electronics. Commercial component availability is resulting in a need for Pb-free components to be incorporated into Sn-Pb assemblies and used for rework. At least three assembly scenarios are possible. The first option is to design for reliable Pb-free components/Sn-Pb solder assembly with process parameters providing the best reliability for mixed assembly. The second option, discussed at length in this paper, is incorporation of one or more Pb-free

components in a Sn-Pb assembly using conventional Sn-Pb process parameters. The third option is to modify the Sn-Pb process for certain configurations to achieve acceptable levels of reliability. A special consideration for high-reliability applications is that Pb-free components may be unintentionally attached with Sn-Pb solder throughout their service life and during repair depot activity.

There is not enough data available on the solder joint reliability of mixed Pb-free components assembled with Sn-Pb solder, and the existing data are inconsistent.<sup>1–12</sup> It is generally believed that it is desirable to have a SAC ball that is completely molten, in order to form a well-mixed alloy upon solidification.

This paper finalizes Celestica's experimental studies on Pb-free ball grid array components assembled using Sn-Pb solder. The program was started in 2002, and consisted of three projects done on three test vehicles: RIA1, RIA2, and RIA3. In this paper, the new reliability data obtained from the RIA3 project will be presented. The data will be compared with the previously published results,<sup>13–17</sup> discussed, and summarized.

(Received May 5, 2008; accepted October 8, 2008; published online November 7, 2008)

## EXPERIMENTAL

The test vehicle RIA3 employed in this study is shown in Fig. 1. This test vehicle is a modification of the RIA2 vehicle,<sup>16</sup> with a change to some component types. The four component types used and their characteristics are shown in Table I. These components were terminated with both SAC305 and SAC405 balls. They were assembled to the cards with Sn-Pb solder paste; therefore, mixed solder joints were formed. All four component types with SAC305 balls were also soldered using SAC305 paste to create a Pb-free cell for comparison.



Fig. 1. Assembled board.

Table I. Component Characteristics

Component	Pitch (mm)	Ball Diameter (mm)
PBGA676	1.0	0.63
PBGA256	1.27	0.75
PBGA196	1.0	0.50
CSP64	0.75	0.46

The boards had 12 layers, with dimensions of 203 mm × 253 mm × 2.36 mm. The test vehicle laminate material was a lead-free compatible material which is designed to withstand the higher temperature requirements of lead-free processing. The surface finish used in this study was organic solderability preservation (OSP).

Three reflow profiles were used in this study, and have been previously described.<sup>16</sup> The low temperature profile temperatures ranged from 203°C in the inner joints of the PBGA676 to 210°C in the CSP64. The peak reflow temperatures in the medium profile were in the 208°C to 210°C range. The high profile temperatures varied from 211°C to 220°C. The times above the Sn-Pb liquidus (TAL) of 183°C were 80 s, 110 s, and 100 s, respectively. The profile characteristics and degree of mixing are shown in Table II. The results in Table II were first reported in McCormick et al.<sup>16</sup>

Assembly was performed using no-clean solder paste in a nitrogen atmosphere, using a ten-zone BTU Conceptronics 150 oven. Prior to population, all cards were preconditioned through the same reflow profile to mimic a double-sided SMT process.

The accelerated thermal cycling (ATC) test setup and failure criteria were described in a previous publication.<sup>16</sup> The profile used was 0°C to 100°C, with a dwell time of not less than 10 min at both high and low temperatures, and 15 min for each of the ramp-up and ramp-down times. The test duration was 6000 cycles. The cards were monitored *in situ* for the entire duration of the test using dataloggers. A total of 16 cards for each cell were tested; each card had two components of each type to bring the total assembled component count to 32. This mixed assembly evaluation was part of a much larger project that included pure SAC305 and SAC405 cells, which allowed a comparison to be made between mixed and pure Pb-free joint reliability. The large number of test vehicles were divided up randomly and placed in one of six chambers. One chamber was started later, and those test vehicles were excluded from this discussion.

Table II. Reflow Profile Characterisation and Degree of Mixing

Reflow Profile	Cell	Ball Metallurgy	Degree of Mixing (%)				
			PBGA676	PBGA256		PBGA196	CSP64
				1st row	4th row		
Low 203–210°C 80 s	1-3	SAC305	30–50	35–40	30	60	65–70
	1-4	SAC405	40–50	40	40–50	50	60
Medium 208–210°C 110 s	1-1	SAC305	45–75	70–85	80–90	50–80	80–90
	1-2	SAC405	40–50	60–70	60–80	60	60–70
High 210–220°C 100 s	1-5	SAC305	60–95	100	90–100	100	100
	1-6	SAC405	70–100	100	90–100	100	100
235–240°C	2-4	SAC305	n/a	n/a	n/a	n/a	n/a

The test was stopped periodically to isolate the failing joints on the failed nets. The test vehicles had been designed to allow BGAs to be cut out from an assembly without damaging the connections to the remaining components on the board. The failure analyses were conducted as soon as possible after the failures occurred. The earliest two cycle failures per component, per each SAC 305 and SAC 405 cell, were cut out for analysis. The boards were then placed back into the chamber, and the first failure joints were cross-sectioned. The latest failures were also cross-sectioned and analyzed to confirm the failure mode. After 6000 cycles, all failed and some surviving BGA joints were subjected to dye-and-pry test analysis.

As-assembled and thermally cycled solder joints were examined using optical microscopy, transmissive x-ray (Phoenix PCB analyzer), scanning electron microscopy (SEM, Hitachi S-4500 and SEM Hitachi S-3000N), and x-ray spectroscopy (Oxford EDX).

Differential scanning calorimetry (TA DSC 2910) analyses were performed to study solder joint melting after partial or complete mixing of the Sn-Pb solder with SAC305 or SAC405 balls during assembly. Several SAC105/Sn-Pb joints were analyzed as well.

## RESULTS AND DISCUSSIONS

### PBGA196

#### Statistical Analysis

In order to compare mixed SAC305 or SAC405 ball/Sn-Pb paste joints assembled using different Sn-Pb thermal profiles with pure SAC305 joints,

Weibull plots were created (Figs. 2 and 3). The number of cycles to 1% failure depending on the solder joint metallurgy is shown in Fig. 3b. It can be seen from Figs. 2a and 3 that pure SAC305 outperforms mixed joints with SAC305 balls. There is a statistically significant difference in the cycle time to 1% failure between pure SAC305 and all three mixed cells. Nevertheless, there are no statistically significant differences in the characteristic life between SAC305 and mixed SAC305/Sn-Pb assembled using low and medium profiles. However, SAC305 performs about two times better than mixed SAC305/Sn-Pb joints assembled using a reflow profile with the highest peak temperature within the conventional temperature range for Sn-Pb assembly. The Weibull slopes  $\beta$  of mixed assemblies are 6.4, 8.5, and 7.6 for low, medium, and high profiles, respectively, and lower than the slope of pure SAC305, which is 12.8.

Mixed solder joints formed with SAC405 components under all three profiles outperform SAC305/Sn-Pb joints significantly in terms of 1% failure and characteristic life (Figs. 2b and 3). For comparison with pure Sn-Pb joints, data from a previous project RIA2 are included in Fig. 3. Both SAC305 and SAC405 mixed joints demonstrate better reliability and higher cycles to 1% failure than do pure Sn-Pb joints formed on an OSP finish.

The same trend of better reliability for lower-temperature assembly was observed for mixed SAC405/Sn-Pb joints. SAC405/Sn-Pb assembled using low and medium reflow profiles have better reliability than SAC405/Sn-Pb assembled at the higher temperature (Figs. 2b and 3). In order to

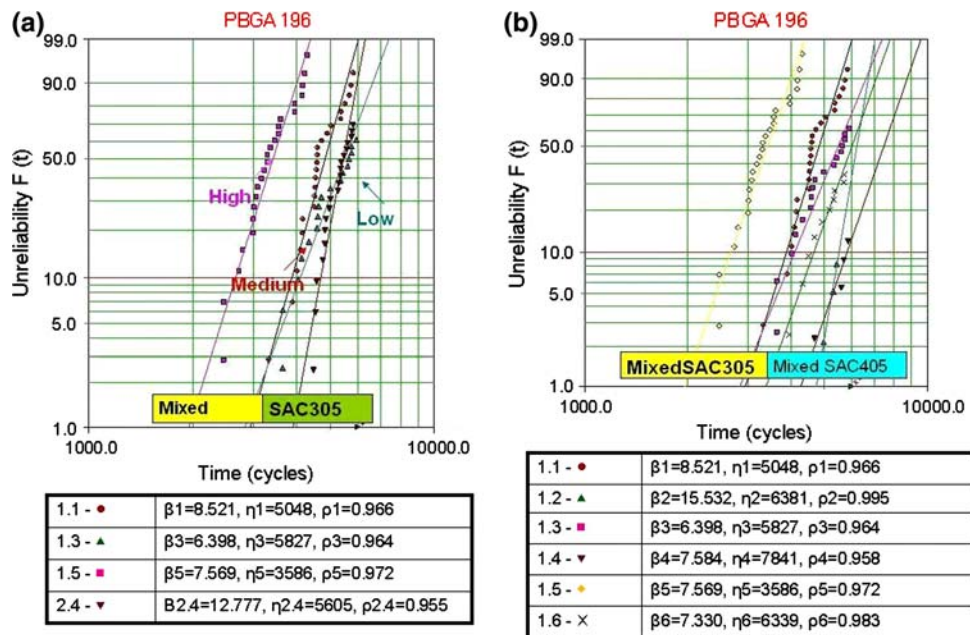


Fig. 2. Weibull plots of PBGA196: (a) comparison of SAC305 ball/Sn-Pb paste mixed joints and pure SAC305 joints and (b) comparison of mixed SAC305 ball/Sn-Pb paste and mixed SAC405 ball/Sn-Pb paste joints. Cells are defined in Table II.



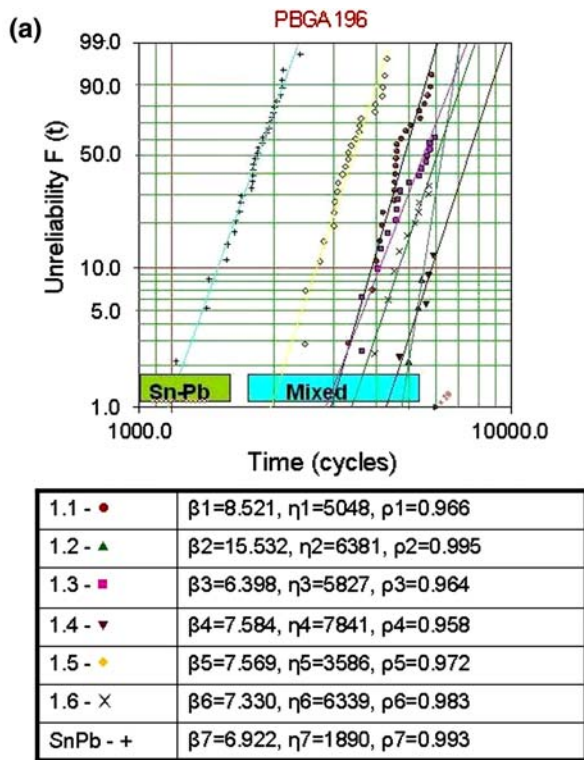


Fig. 3. Thermomechanical reliability of PBGA196 with different solder joint composition assembled using low (L), medium (M), and high (H) reflow profiles: (a) Weibull plots and (b) cycles to 1% failure. Cells are defined in Table II.

understand this behavior, detailed microstructural analyses were performed.

*As-Assembled Microstructure*

X-ray inspection did not show any defects except for some voiding that was at an acceptable level for all cells. The joints were properly shaped and self-aligned except cell 1-1 (Fig. 4). There was no difference in standoff between corner and centre joints measured on diagonal cross-sections. There is a difference in standoff between the cells, but there is no direct correlation between the heights of the joints and their resulting reliability. Although the joints of cell 1-6 (394 μm) are higher than those of

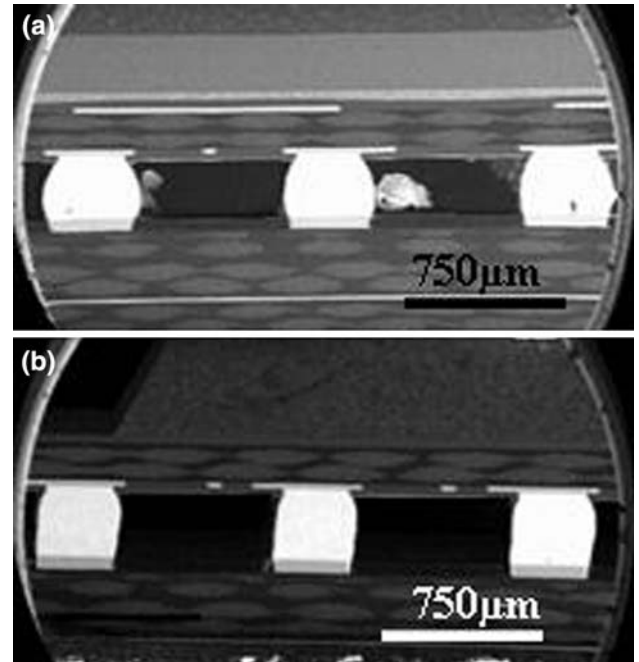


Fig. 4. Cross-sections of PBGA196: (a) cell 1-2, SAC405 ball/Sn-Pb paste and (b) cell 1-1, SAC305 ball/Sn-Pb paste; SEM, 20×. Cells are defined in Table II.

cells 1-2 (383 μm) and 1-4 (384 μm), the reliability of the latter two cells is better. The cycles to failure of cells 1-1 and 1-3 are almost the same, but the standoff of cell 1-1 joints is 19% larger than for cell 1-3 (445 μm and 374 μm, respectively).

Both SAC305/Sn-Pb and SAC405/Sn-Pb joints assembled using low and medium profiles were 50% to 80% mixed, as exemplified in Fig. 5a. The microstructure of partially mixed joints contains a SAC305 or SAC405 solder ball portion with an unchanged microstructure, and a portion of mixed solder. The theory of mixing of lead-free balls with Sn-Pb solder is described in Ref. 18. When Sn-Pb solder melts at 183°C, the SAC ball begins to dissolve in the liquid solder, enriching it with Ag and Sn. The percentage of Pb thereby decreases. The microstructure of the mixed part is not uniform. The area adjacent to the remaining solder ball consists of a wide Sn band that has a dendritic shape (Fig. 5b, c). A small amount of Pb and intermetallic particles are situated between the Sn dendrite arms. (A detailed study on Sn band formation was performed on different mixed joint metallurgies and will be published in a future paper.)

There were no visible portions of the initial solder ball left in solder joints assembled using high reflow profiles, as shown in Fig. 6a. Therefore, they were marked as 100% mixed in Table II. In-depth analysis showed that the microstructure of what we called “fully” or 100% mixed joints is not uniform. The top layer adjacent to the component contains more Sn-primary dendrites, and their arms are larger in size than in the rest of the joint (Fig. 6b). The Pb fraction is also higher. Very narrow

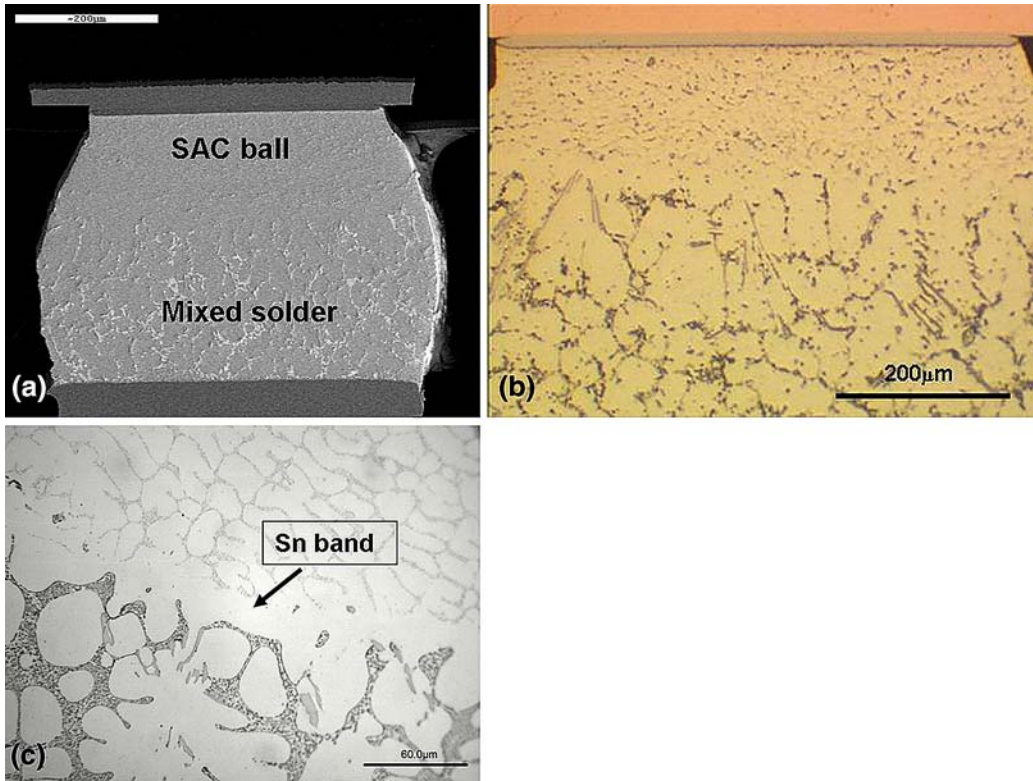


Fig. 5. A typical microstructure of a partially mixed solder joint: cell 1-3, SAC305 ball/Sn-Pb paste, SEM at (a) 180 $\times$  and (b) 200 $\times$ ; (c) SAC105 ball/Sn-Pb paste. Cells are defined in Table II.

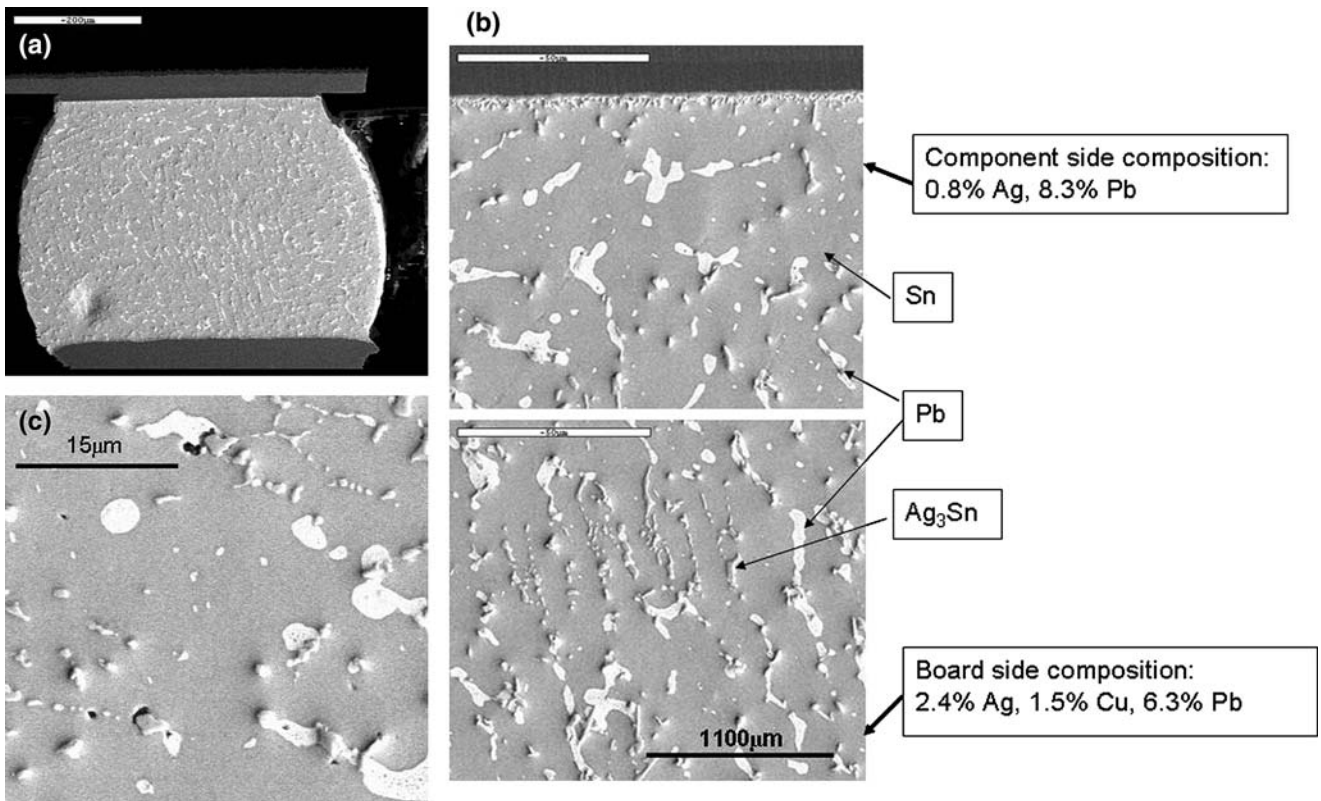


Fig. 6. A typical microstructure of a fully mixed solder joint showing that, even if the ball is completely dissolved in solder, the microstructure may be still nonuniform: cell 1-5, SAC305 ball/Sn-Pb paste, SEM: (a) no visible portions of the initial solder ball, 180 $\times$ ; (b) nonuniform composition and phase distribution across the joint, 1100 $\times$ ; and (c) microstructure details with shrinkage voids, 2000 $\times$ .

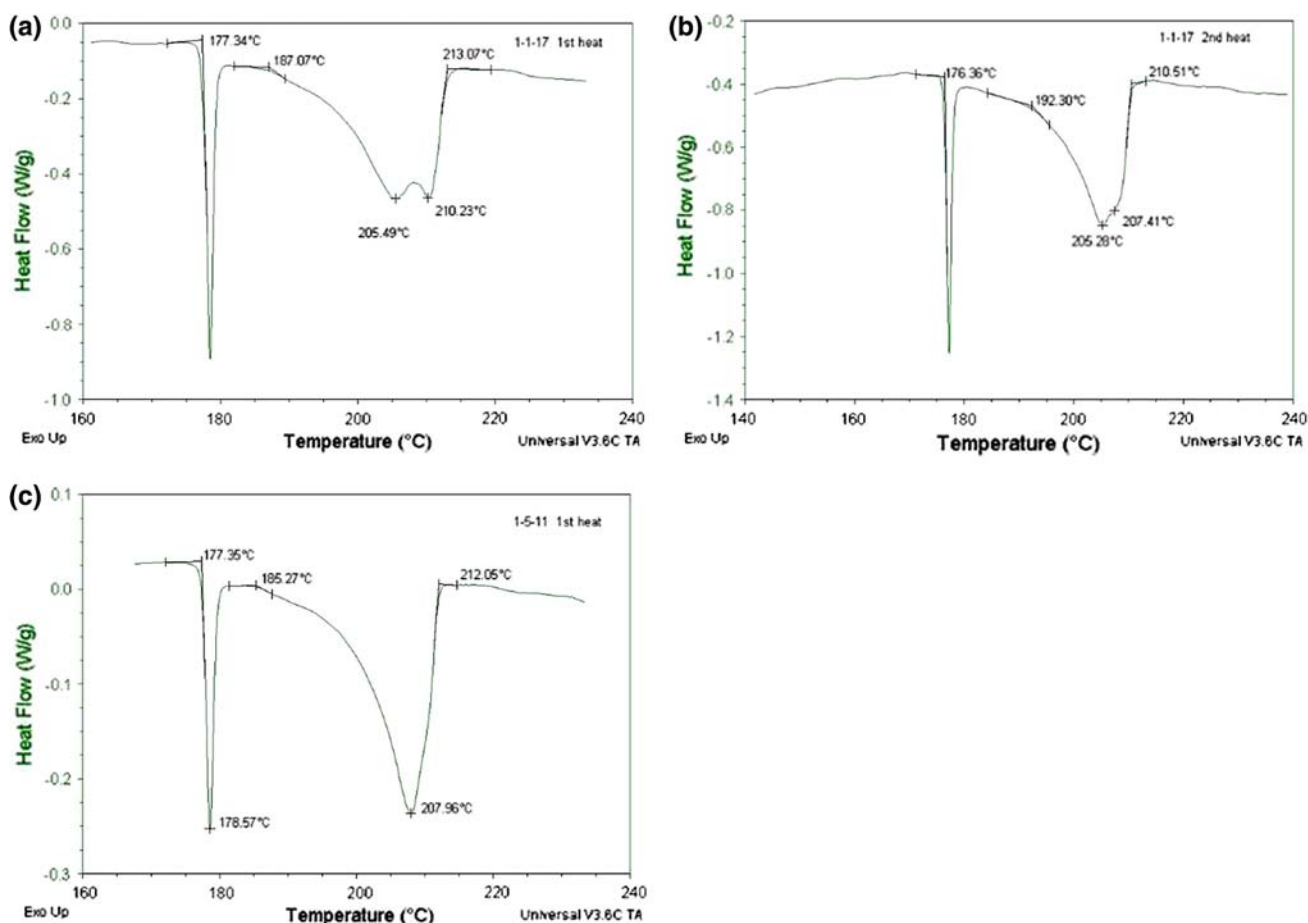


Fig. 7. DSC heating curves for SAC305 ball/Sn-Pb paste solder joints: (a) cell 1-3, first run, low reflow profile; (b) cell 1-3, second run, low reflow profile; and (c) cell 1-5, first run, high reflow profile. Cells are defined in Table II.

interdendritic spaces are occupied by  $\text{Ag}_3\text{Sn}$  particles, and often contain small shrinkage voids (Fig. 6c). This microstructure is quite similar to the band adjacent to the remaining ball in incompletely mixed joints (Fig. 5b, c). This imperfection is less visible in SAC405/Sn-Pb joints assembled using a high reflow profile. It also was not detected in the previous RIA2 project, where profiles with 215°C and 220°C minimum temperatures were used.

In order to understand the microstructure formation during solidification, DSC analyses were performed on all PBGA196 cell samples at time zero. The samples were heated at 5°C/min to 240°C, cooled, and reheated. Representative curves are shown in Fig. 7. The joints assembled using low and medium profiles continued mixing during the first DSC heating run, as is illustrated by the change in the melting maximum above 205°C from Fig. 7a to 7b. The second run curves are very similar to the first heating run of high temperature reflow profile samples, with complete mixing at 207°C (Fig. 7c). There is no significant difference between the first and second heating of the high profile samples, as full mixing occurs during reflow. The temperature for complete mixing of PBGA196 joints is about 207°C, which corresponds with what Handwerker

reported based on a thermodynamic model.<sup>19</sup> The pasty range of mixed PBGA196 joints is not less than 30°C.

The DSC curves reveal that ternary eutectic Sn +  $\text{Ag}_3\text{Sn}$  + Pb (m.p. 177°C), binary eutectic Sn + Pb, and primary Sn crystals (melting over 205°C) are present in the joints. The melting of the small remaining amount of binary Sn + Pb is masked by the wide pasty range. The difficulties of  $\beta$ -Sn nucleation<sup>20</sup> that result in high undercooling in SAC solders are overcome by the presence of a Sn phase in the remaining portion of the solder ball. Solidification of the mixed solder portion in a partially mixed joint starts with the primary Sn formation. It starts growing from the existing Sn, forming a dendritic band as shown in Fig. 5. This band is more likely monocrystalline, because once  $\beta$ -Sn nucleation commences, solidification is so rapid that there is almost no time left for additional  $\beta$ -Sn nuclei to form. Then the binary Sn + Pb eutectic crystallizes in the interdendritic spaces, followed by the ternary Sn +  $\text{Ag}_3\text{Sn}$  + Pb eutectic. Even in the case of a high temperature profile where the undissolved SAC ball portion is not visible, some remaining Sn species or Sn clusters may be available for nucleation. This Sn availability may explain



the nonuniform microstructure of fully mixed joints formed during a conventional Sn-Pb profile.

#### Microstructure after ATC

Both partially and fully mixed SAC305/Sn-Pb and SAC405/Sn-Pb PBGA196 joints have package-side failure, as shown in Fig. 8. Cracks propagate through the solder along the component pad intermetallic layer. Since for partially mixed solder joints this region is essentially pure SAC305 or SAC405 (Fig. 8a), the details of crack propagation and failure mechanism are the same as for pure lead-free PBGA196, and were described by the authors in Ref. 18. The difference in microstructure<sup>18</sup> between SAC305 and SAC405 is responsible for the better reliability of SAC405/Sn-Pb joints. In fully mixed joints formed at the high temperature limit of conventional Sn-Pb reflow, cracks propagate through the region containing more Sn and less intermetallic particles than the rest of the solder joint. The Sn is recrystallized, and the small Pb particles precipitate at the boundaries. There are some larger Pb grains in the structure as well. The crack propagates along the grain boundaries, and between the Sn and Pb grains (Fig. 8b, c). The reinforcing effect of Ag<sub>3</sub>Sn and Cu<sub>6</sub>Sn<sub>5</sub> particles is reduced, compared with the

pure SAC region in partially mixed joints (Fig. 8a) and with the uniform microstructure of completely mixed joints formed at temperatures above conventional Sn-Pb profiles (Fig. 8d). These differences in the microstructure uniformity are thought to be the cause of the difference in performance between partially and fully mixed joints.

#### CSP64

The results of thermal cycling after the completion of 6000 cycles are shown in Table III. The data from the pure SAC305 cell 2-4 are included for comparison. No failure was detected in mixed cell 1-3 and pure SAC305, and only one failure out of 24 tested components occurred in each of the remaining cells. The lowest number of cycles to first failure was greater than 4000 cycles, and happened in cell 1-5 assembled using the high temperature profile. The failure mode and DSC data were similar to those of PBGA196.

#### PBGA676 and PBGA256

The cycles to failure after the completion of 6000 cycles are shown in Table III. No failure was detected in mixed and pure SAC PBGA256 joints

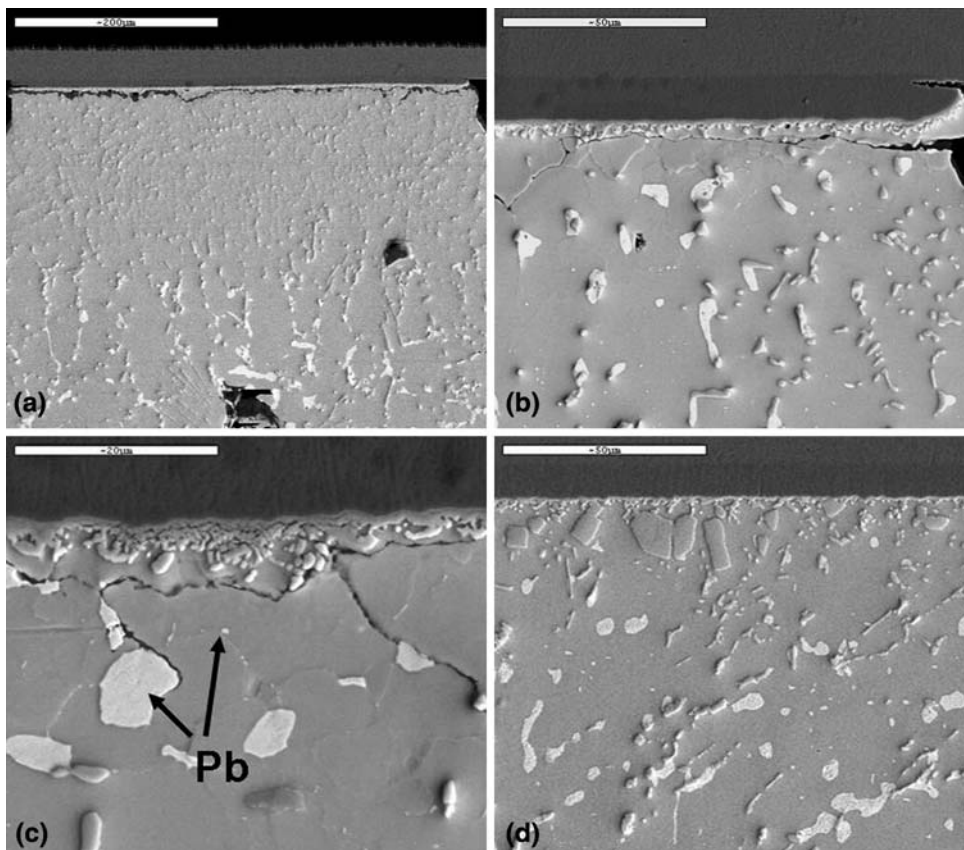


Fig. 8. PBGA196 microstructure after thermal cycling, 0°C to 100°C cycling, SEM: (a) cell 1-3, SAC305 ball/Sn-Pb paste, 250×; (b) cell 1-3, SAC305 ball/Sn-Pb paste, 1000×; (c) cell 1-5, SAC305 ball/Sn-Pb paste, 250×; and (d) cell 1-6, SAC405 ball/Sn-Pb paste, 1000×. Cells are defined in Table II.

**Table III. Failures after 6000 Cycles at 0°C to 100°C**

Component	Low Reflow Profile		Medium Reflow Profile		High Reflow Profile		Lead-Free Cell
	1-3	1-4	1-1	1-2	1-5	1-6	
CSP64	No	4719	5012	4493	4475	5432	No
PBGA256	No	5426	No	No	No	No	No
PBGA676	No	5643	4344	No	5665	4484; 4849	5136; 5299; 5408

except cell 1-4, where the first failure was found at 5426 cycles.

The maximum number of failures in mixed PBGA676s was two, in cell 1-6. Joints from cells 1-2 and 1-3 withstood 6000 cycles without failure. Pure SAC305 demonstrated three closely spaced failures above 5000 cycles. Comparing data from cell 1-6 to 2-4 allows us to conclude that a mixed cell Weibull plot will appear consistent with PBGA196 plots. The cycles to failure in cell 1-6 are 4484 and 4849, with no more failures up to 6000 cycles.

The microstructure of the solder joints across the PBGA676 is nonuniform. The centre joints are 70% mixed, whereas the corner joints are fully mixed. The microstructure of these mixed joints varies from the component side to the board side, and is similar to what was described for PBGA196 (Fig. 6). The layer adjacent to the component contains a Sn-rich band that provides an easy route for crack propagation. The crystallographic orientation of Sn dendrites may also play a significant role in the thermal fatigue resistance. Disadvantageously oriented joints would be more prone to early fatigue failure than would other joints. We observed this situation in the RIA2 project when SAC405 CBGA937 components were assembled using Sn-Pb solder with a 215°C profile.<sup>18</sup> The degree of mixing was close to that of PBGA676 in this study. The  $\beta$  slope was 2.8, compared with 12.8 for completely mixed joints with a uniform microstructure assembled with a 220°C profile, and 15.2 for a pure SAC405 assembly.

It is very important to stress that, in the Celestica RIA studies, the root cause of all failures in all types of SAC ball/Sn-Pb paste joints, independent of the degree of mixing, was crack propagation through bulk solder on the component side. Secondary cracks were observed on the board side, but as they were partial cracks, they did not result in electrical failure.

## Defects and Anomalies

### Interfacial Failure

Unlike the data obtained in Celestica RIA projects, there are data reported in the literature on interfacial failure in mixed joints.<sup>1,2,5,11</sup> We also observed this type of failure working with our customers on their assemblies, and in consortium projects. Some of the data were published<sup>15,16</sup> and some

will be published soon. It was found that mixed assemblies, either partially or fully mixed, very often fractured interfacially at the board side after ATC. This failure mode more often occurs on electroless nickel immersion gold (ENIG) or electrolytic Ni/electrolytic Au finishes, but may happen on OSP, immersion Sn, and immersion Ag as well. The crack propagates between the intermetallic layer and the solder (Fig. 9a). Detailed examination of the as-assembled microstructure (Fig. 9b) and early stages of crack formation (Fig. 9c) reveals that it follows the ternary Sn + Ag<sub>3</sub>Sn + Pb and/or quaternary Sn + Ag<sub>3</sub>Sn + Cu<sub>6</sub>Sn<sub>5</sub> + Pb eutectic that accumulates at the board side (Fig. 9b, c). The crack also penetrates into interdendritic spaces occupied by the eutectic.

The accumulation of the low melt eutectic at the board side relates to a temperature gradient across the solder joint, with the Cu pads as the hottest place. Mixed solder joints have a very wide pasty range. For PBGA196, the range is 30°C, between 207°C and 177°C (Fig. 7), where 177°C is the melting point of a ternary eutectic. The pasty range is even wider for joints with larger solder balls and a lower relative volume of solder paste. The presence of Au results in an additional depression of the lower temperature. During reflow cooling, solidification begins at the coldest location with Sn nucleation and growth in a dendritic shape towards the hot board side. The liquid, which is gradually being enriched by Pb and Ag and depleted of Sn, finally crystallizes as binary and then ternary eutectic in interdendritic spaces. The last portion of liquid will solidify as a ternary eutectic at the board side when the temperature of that region reaches about 177°C.

Any additional constituents resulting from dissolution of substrate material, such as Au in the joints formed on Ni/Au finished pads, will segregate in the last liquid to freeze, reducing the eutectic temperature even further. Impurities from solder paste and solder ball that are not dissolved in solid Sn will be concentrated in this region as well. The concentration of solder contamination may exceed acceptable levels, causing dewetting, oxidation, and degradation of mechanical properties. Shrinkage voids will be formed in the last portion of liquid as well. Therefore, the interface between the Cu or Ni reaction intermetallic layer and bulk solder may be insufficiently strong to withstand stresses



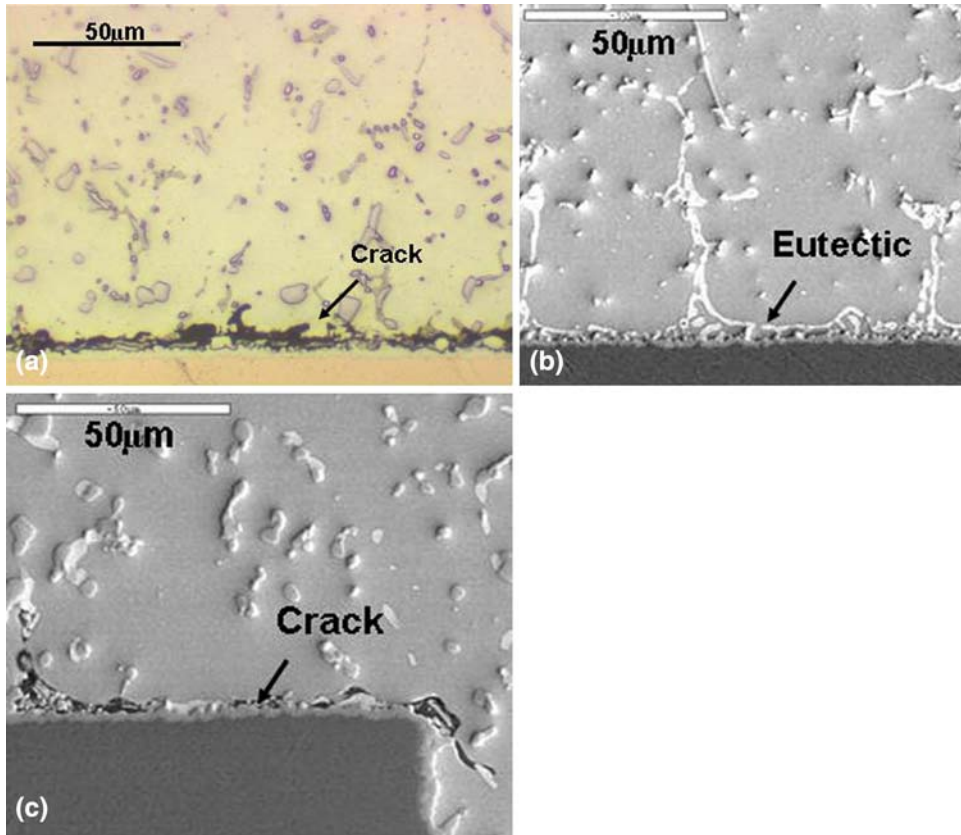


Fig. 9. Interfacial cracks in SAC305 ball/Sn-Pb paste joints: (a) after ATC, 200 $\times$ ; (b) as-assembled,<sup>15</sup> SEM, 1000 $\times$ ; and (c) after ATC, SEM 1000 $\times$ .

experienced during thermomechanical testing. It is believed that reducing the temperature difference across the solder joints, increasing the cooling rate, and choosing a solder paste with lower concentrations of trace elements will help to reduce the propensity of mixed solder joints to interfacial failure.

#### Rework Defect

The mechanism described above is also responsible for mixed assembly rework defect that looks like a crack at the component side (Fig. 10a). This type of defect cannot be detected electrically, but will cause a significant reduction in the thermomechanical fatigue life. This defect is more typical for SAC105/Sn-Pb joints that have a 40°C pasty range (Fig. 10b), which is 10°C wider than the range for SAC305/Sn-Pb for the same solder ball/solder paste mass ratio. This defect is very difficult to avoid, especially if the board is thick, as the board may be colder than the component side because of the top-side heating conditions during rework. The crystallization starts from the board side, and heat dissipation occurs through the cold board. The Sn dendrites grow towards the component side, pushing the liquid to the Cu pad. Because most of the solder joint is already solid, the contraction forces may also play a significant role in opening the gap through the liquid layer. A close look shows the

eutectic layer at the pad/solder interface (Fig. 10a). The separation has a dendritic shape resulting from the eutectic on the pad surface and between the dendritic arms.

A wide pasty range may also cause problems with secondary reflow of backside components during double-sided assembly, and rework and neighboring components during rework.

#### SUMMARY AND CONCLUSIONS

The following summarizing conclusions are based on Celestica studies published in this and in previous papers.

The ATC reliability of SAC ball/Sn-Pb paste joints strongly depends on microstructure. The mixed assembly microstructure could be divided into three categories:

1. Completely mixed with uniform microstructure.
2. Completely mixed with nonuniform microstructure: the Sn-enriched zone is visible.
3. Partially mixed joints where the remains of solder balls with initial SAC305 or SAC405 ball structure are present. None of the joints in the component are mixed more than 80%.

The fatigue life of categories 1 and 3 is sufficient and comparable to pure Sn-Pb and lead-free fatigue lives. The microstructure of category 1 may be

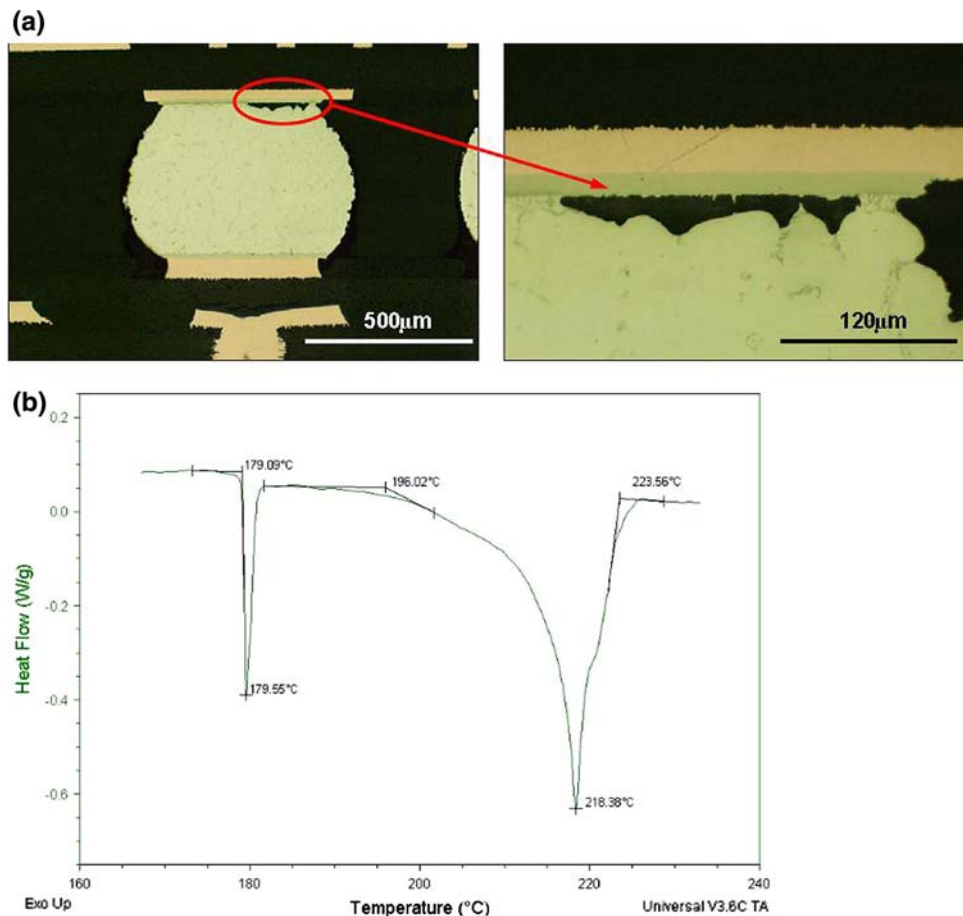


Fig. 10. (a, b) Shrinkage voids formed in the reworked solder joint and (c) DSC curve of a SAC105 ball/Sn-Pb paste joint showing a wide pasty range.

described as Sn-Pb reinforced with  $\text{Ag}_3\text{Sn}$  particles. In category 3, cracks propagate through the unmixed lead-free solder portion, which should not be significantly different from pure lead-free joints. The slightly reduced reliability for category 3 that was observed in the present study may be explained by some additional coefficient of thermal expansion (CTE) mismatch of the two solders. The reliability of category 2 is lower compared with that of categories 1 and 3, and the nonuniform microstructure with Sn-band may result in early failures and a very low  $\beta$  slope. This microstructure should be avoided.

To provide optimum properties for mixed SAC ball/Sn-Pb paste joints, the reflow parameters should be carefully considered. The following gradation is proposed:

1. *Mixed assembly reflow that is designed intentionally for backward compatibility.* The minimum reflow temperature of this profile should be above  $220^\circ\text{C}$  to achieve full mixing with uniform microstructure across the joints in all components in the assembly. The board and components should be lead-free compatible and able to withstand high temperature. With these conditions, the ATC reliability of mixed solder joints is

comparable to that of Sn-Pb or better, depending on the component type.

2. *Conventional Sn-Pb reflow in the range of  $205^\circ\text{C}$  to  $220^\circ\text{C}$ .* This type of reflow may produce all three categories of mixed assembly microstructures. Therefore, there is a risk of early failures. In addition, although partial mixing is acceptable for many components with extended reliability, some highly stressed ceramic components will not have the required level of reliability in the partially mixed form. If a conventional Sn-Pb profile is chosen, additional validation and qualification are always required. The lead-free components with known behavior in mixed assembly, which were analyzed in this and other programs, may be successfully incorporated in Sn-Pb assembly with Sn-Pb process compatible boards and components.

The process window for SMT and rework is narrower because of the wide melting and solidification range of mixed solder joints. It is important to control the assembly parameters so that the temperature gradient and cooling rate across the joints are more uniform. This will mitigate the potential for generating interfacial failure. Rework of low-Ag alloys such as SAC105 requires even more precautions,

and may not be possible in some cases such as for thick boards, mirrored components, and high-density assembly.

The allowable trace-element level may need tighter control for low-Ag SAC alloys. A lower Ag content results in segregation of impurities and trace elements at the interfaces when the last liquid freezes.

### ACKNOWLEDGEMENTS

The authors would like to thank the following individuals from Celestica, Toronto: Blake Harper for statistical analysis and Thilo Sack for technical discussions and paper review. The authors thank the Celestica Thailand Lab for the rework analysis and images.

### REFERENCES

1. P.T. Vianco and J. Rejent, *Proceedings of the 46th Electronics Components and Technology Conference* (Piscataway, NJ: IEEE, 1966), p. 283.
2. Q. Zhu, M. Sheng, and L. Luo, *Solder. Surf. Mt. Technol.* 12, 19 (2000). doi:[10.1108/09540910010347854](https://doi.org/10.1108/09540910010347854).
3. C. Handwerker, J. Bath, E. Benedetto, E. Bradley, R. Gedney, T. Siewert, P. Snugovsky, and J. Sohn, *Proceedings of the SMTA International Conference* (Edina, MN: SMTA, 2003), p. 664.
4. F. Hua, R. Aspandiar, C. Anderson, G. Clemons, C.K. Chung, and M. Faizul, *Surf. Mt. Technol.* 16, 1–34 (2003).
5. D. Hillman, M. Wells, and K. Cho, *Proceedings of the CMAP International Conference on Lead-Free Soldering*, Toronto, Canada (2005).
6. B. Nandagopal, D. Chiang, S. Teng, P. Thune, L. Anderson, R. Jay, and J. Bath, *Proceedings of the SMTA International Conference* (Edina, MN: SMTA, 2005), pp. 861–870.
7. J. Bath, S. Sethuraman, X. Zhou, D. Willie, K. Hyland, K. Newman, L. Hu, D. Love, H. Reynolds, K. Kochi, D. Chiang, V. Chin, S. Teng, M. Ahmed, G. Henshall, V. Schoeder, Q. Nguyen, A. Maheswari, M. Lee, J.P. Clech, J. Cannis, J. Lau, and C. Gibson, *Proceedings of the SMTA International Conference* (Edina, MN: SMTA, 2005), p. 568.
8. I. Chatterji, *Proceedings of the SMTA International Conference* (Edina, MN: SMTA, 2006), p. 416.
9. M. Abtew, R. Kinyanjui, N. Nuchsupap, T. Chavasiri, N. Yingyod, P. Saetang, J. Krapun, and K. Jikratoke, *Proceedings of the SMTA International Conference* (Edina, MN: SMTA, 2006), p. 376.
10. J. Nguyen, D. Geiger, D. Rooney, and D. Shangguan, *Proceedings of IPC Printed Circuits Expo, APEX Conference* (2006), p. 433.
11. G. Henshall, P. Roubaud, G. Chew, S. Prasad, F. Carson, R. Bulwith, and E. O’Keeffe, *Proceedings of the SMTA International Conference* (Edina, MN: SMTA, 2003), p. 245.
12. A.R. Zbrzezny, P. Snugovsky, R. Lau, and T. Lindsay, *IEEE Trans. Electron. Packag. Manuf.* 29, 211 (2006). www.CPMT.org (ISSN 1521-334X).
13. P. Snugovsky, M. Kelly, Z. Bagheri, and M. Romansky, *Proc. IPC*, Brussels (2003).
14. P. Snugovsky, Z. Bagheri, and M. Kelly, *Proceedings of the SMTA International Conference* (Edina, MN: SMTA, 2002), p. 823.
15. P. Snugovsky, A.R. Zbrzezny, M. Kelly, and M. Romansky, *Proceedings of CMAP International Conference on Lead-Free Soldering*, Toronto, Canada (2005).
16. H. McCormick, P. Snugovsky, Z. Bagheri, S. Bagheri, C. Hamilton, G. Riccitelli, and R. Mohabir, *J. Surf. Mt. Technol.* 20, 2–11 (2007).
17. S. Bagheri, P. Snugovsky, Z. Bagheri, M. Romansky, M. Cole, M. Kelly, M. Interrante, G. Martin, C. Bergeron, M. Farooq, and M. Hoffmeyer, *J. Surf. Mt. Technol.* 19, 4–18 (2006).
18. P. Snugovsky, Z. Bagheri, H. McCormick, S. Bagheri, C. Hamilton, and M. Romansky, *J. Surf. Mt. Technol.* 20, 3–17 (2007).
19. C. Handwerker, *Circuits Assembly*, March 2005, p. 39.
20. D. Swenson, *J. Mater. Sci. Mater. Electron.* 18, 39 (2006). doi:[10.1007/s10854-006-9012-8](https://doi.org/10.1007/s10854-006-9012-8).